

^a

MUCH ADO ABOUT NOTHING: VACUUM AND RENORMALIZATION ON THE LIGHT-FRONT

Matthias Burkardt

*Department of Physics, New Mexico State University,
Las Cruces, NM 88003-0001, USA*

In the first part of my lectures, I will use the example of deep-inelastic scattering to explain why light-front coordinates play a distinguished role in many high energy scattering experiments. After a brief introduction into the concept of light-front quantization, I will show that the vacuum for any light-front Hamiltonian is trivial, i.e. the same as for non-interacting fields. In the rest of my lectures, I will discuss several toy models in 1+1 and 3+1 dimensions and discuss how effective light-front Hamiltonians resolve the apparent paradox that results from having a trivial light-front vacuum.

1 The Uses of Light-Front Quantization

^b In deep-inelastic scattering (DIS) experiments one scatters leptons at very high energy from a nucleon or a nucleus. Typically, the target nucleon gets destroyed in such a process and one obtains a large number of particles in the final state. In the most simple version of these experiments (inclusive), one completely ignores all the details of the hadronic final state and only measures the energy transfer $\nu = E - E'$ and momentum transfer $Q^2 = -q^2$ from the lepton on the target. The double differential (inclusive) cross section for the scattering angle and energy of the lepton can be written in the form

$$\frac{d^2\sigma}{d\Omega dE'} = \frac{4\pi\alpha^2}{MQ^4} \left\{ W_2(Q^2, \nu) \cos^2 \frac{\theta}{2} + 2W_1(Q^2, \nu) \sin^2 \frac{\theta}{2} \right\}. \quad (1)$$

In Eq. (1) the Rutherford cross section has been factored out since it represents what one obtains for scattering from point-like targets. ^c In this expression, all details from the microscopic structure of the target are parameterized in the structure functions W_1 and W_2 . In general, i.e. for arbitrary momentum transfer, these structure functions are functions are independent functions of two variables, ν and Q^2 . However, in the Bjorken limit, i.e. when $Q^2 \rightarrow$

^aLecture notes, based on three lectures given at the NUClear Summer School NUSS 97, at Seoul National University, Seoul, South Korea, May 1997.

^bThis Section has been taken from Ref. ¹.

^cFor a point-like target, the structure functions are just δ functions due to energy conservation.

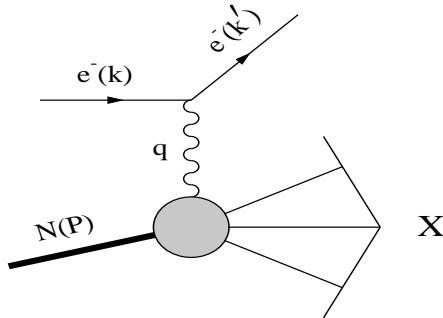


Figure 1: DIS from a nucleon or nucleus. Only the scattered lepton is measured.

∞ and $\nu \rightarrow \infty$, such that $x \equiv Q^2/2M\nu$ fixed, it turns out that to a good approximation W_1 depend only on the ratio $Q^2/2M\nu$

$$\begin{aligned} 2MW_1(Q^2, \nu) &\xrightarrow{Bj} F_1(x) \\ \nu W_2(Q^2, \nu) &\xrightarrow{Bj} F_2(x). \end{aligned} \quad (2)$$

This scaling behavior was the first direct evidence for point-like charged constituents inside the proton, the quarks, and in the parton model one describes hadrons as an ensemble of free quarks and gluons, parameterized by the parton distribution functions which are essentially the Bjorken-scaled structure functions.

These parton distribution functions contain an immense wealth of information about the quark and gluon structure of nucleons and nuclei. However, before one can relate this information to phenomenological models or theoretical calculations, it is essential to understand what these parton distributions really are.

For this purpose, we first use the optical theorem to rewrite the inclusive lepton-nucleon cross section in terms of the imaginary part of the forward Compton amplitude (Fig. 2). In general, i.e. when Q^2 is not large, the two photons in Fig. 2 can couple either to the same quark or to different quarks. However, in the Bjorken limit, it is very difficult for the transferred momentum to flow from the first quark-photon vertex to the second — unless the two photons couple to the same quark. If the two photons couple to different quarks then one needs additional gluons to exchange the momentum and for this one has to “pay” with additional energy denominators. Therefore, for large Q^2 , the crossed diagrams can be omitted.

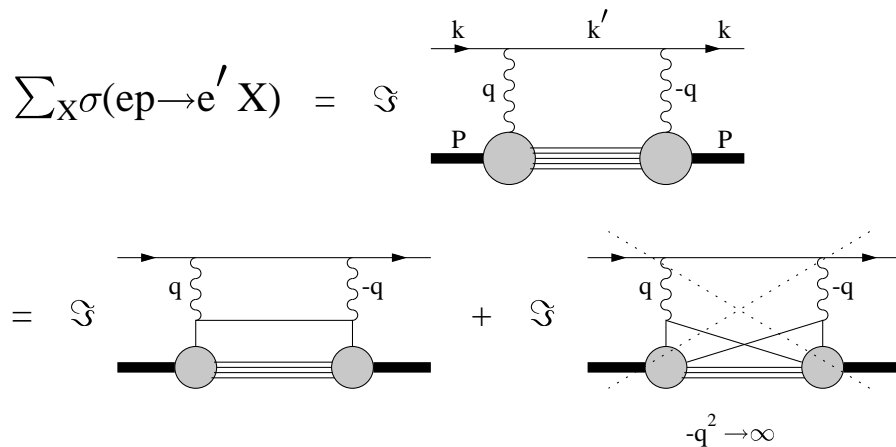


Figure 2: Using the optical theorem to relate the inclusive electron nucleon cross section to the imaginary part of the forward Compton amplitude.

In addition, since QCD is asymptotically free (i.e. the strong coupling constant $\alpha_s(Q^2)$ vanishes for $Q^2 \rightarrow \infty$), one can neglect all interactions of the struck quark when it propagates between the two quark-photon vertices. Finally, since the struck quark is ultra-relativistic (and on its mass shell since we take the imaginary part!) it propagates almost along a light-like direction $x^\mu x_\mu = 0$.

In summary, since the quark does not interact and moves along a light-like direction between the two quark-photon vertices, it is as if one removes the quark at a certain point from the proton and puts it back in at another point which is displaced from the first vertex by a light-like distance. It should therefore not be surprising that the parton distributions measured in DIS are related to correlation functions along a light-like direction:

$$q(x) = \int \frac{d\zeta^-}{2\pi} \langle P | \bar{q}(0) \gamma^+ q(\zeta^-) | P \rangle e^{i\zeta^- x P^+}. \quad (3)$$

It is instructive to compare DIS in non-relativistic systems (e.g. in solid state physics) to the relativistic DIS which we discussed above. The essential difference is that in non-relativistic systems, if the momentum transfer is much larger than the intrinsic momentum scale of the constituents in the target, the struck particle moves much faster than the spectators. As a result, its motion can be approximated as infinitely fast, i.e. instantaneous and one finds

that DIS in non-relativistic systems probes equal time correlation functions: ordinary momentum densities. In contrast, in relativistic systems where both the struck particle and the “spectators” have velocities that are of the order of the speed of light and therefore, the motion cannot be approximated as instantaneous and one probes correlations in a light-like direction: light-front momentum densities.

This means that in a conventional framework, i.e. when x^0 is time, parton distributions are related to real time response functions. In order to calculate them it is not sufficient to know the ground state wave function of the target, but one also needs to know the couplings to excited states as well as the time evolution of the excited states between the two couplings to external photons. This makes it not only difficult to calculate parton distributions but also to interpret them.

The situation changes immediately when one introduces a new time variable $x^+ \equiv x^0 + x^3$ (where x^3 is the direction of the momentum transfer). With this choice of time, light-like correlation function (more precisely: correlation functions in the $x^- = x^0 - x^3$ direction) are equal “time” correlation functions. First of all, it is much easier to calculate in this framework since parton distribution functions are simply momentum densities and it is sufficient to know the ground state LF-wave function in order to compute them. More importantly, since parton distributions are such simple observables, it is much easier to develop an intuitive understanding of otherwise obscure results.

There are many other examples of high energy scattering experiments where LF coordinates also play a distinguished role, such as certain exclusive reactions at large momentum transfer. Some of these will be covered in Stan Brodsky’s lecture notes.

If one wants to take advantage of these results, it is necessary to formulate QCD in a Hamiltonian framework where x^+ is time. What this means will be discussed in Section 2. Quantizing on equal x^+ hypersurfaces is not a new idea. The first work in this direction was by Dirac in 1949².

LF quantization is very similar to canonical equal time (ET) quantization. Both are Hamiltonian formulations of field theory, where one specifies the fields on a particular initial surface. The evolution of the fields off the initial surface is determined by the Lagrangian equations of motion. The main difference is the choice of the initial surface, $x^0 = 0$ for ET and $x^+ = 0$ for the LF respectively. In both frameworks states are expanded in terms of fields (and their derivatives) on this surface. Therefore, the same physical state may have very different wavefunctions^d in the ET and LF approaches because fields at $x^0 = 0$ provide a different basis for expanding a state than fields at $x^+ = 0$.

^dBy “wavefunction” we mean here the collection of all Fock space amplitudes.

The reason is that the microscopic degrees of freedom — field amplitudes at $x^0 = 0$ versus field amplitudes at $x^+ = 0$ — are in general quite different from each other in the two formalisms.

This difference in the choice of microscopic degrees of freedom is what explains how it is possible that a given physical observable (e.g. parton distributions) may be a very complicated object in the ET framework, and at the same time be a relatively simple quantity in the LF framework.

2 Canonical Quantization in Light-Front Coordinates

In this chapter, the formal steps for quantization on the light-front are presented.^e For pedagogical reasons this will be done by comparing with conventional quantization (with x^0 as “time”). On the one hand this shows that the basic steps in the quantization procedure in LF and in ET formalism are in fact very similar. More importantly, however, we will thus be able to highlight the essential differences between these two approaches to quantum field theory more easily.

In the context of canonical quantization one usually starts from the action

$$S = \int d^4x \mathcal{L}. \quad (4)$$

($\mathcal{L} = \mathcal{L}(\phi, \partial_\mu \phi)$) After selecting a time direction τ ^f one forms the momenta which are canonically conjugate to ϕ

$$\Pi(x) = \frac{\delta \mathcal{L}}{\delta \partial_\tau \phi} \quad (5)$$

and postulates canonical commutation relations between fields and corresponding momenta at equal “time” τ (Table 1).^g

In the next step one constructs the Hamilton operator and the other components of the momentum vector. Thus one has completely specified the dynamics and can start solving the equations of motion. Typically, one either makes some variational ansatz or a Fock space expansion. In the latter approach one writes the hadron wave function as a sum over components with a fixed number of elementary quanta (for example in QCD: $q\bar{q}$, $q\bar{q}q\bar{q}$, $q\bar{q}g$, e.t.c.). The expansion coefficients, i.e. the wavefunctions for the corresponding Fock

^eFor a more detailed discussion, see the recent review in Ref. ³.

^fHere τ may stand for ordinary time x^0 as well as for LF time $x^+ = (x^0 + x^3)/\sqrt{2}$ or any other (not space-like) direction.

^gThe canonical quantization procedure in the ET formulation can for example be found in Ref. ⁴. The rules for canonical LF-quantization have been taken from Refs. ⁵.

normal coordinates	light-front
coordinates	
x^0 time	$x^+ = \frac{x^0 + x^3}{\sqrt{2}}$ time
x^1, x^2, x^3 space	$x^- = \frac{x^0 - x^3}{\sqrt{2}}, x^1, x^2$ space
scalar product	
$a \cdot b = a^0 b^0 - \vec{a} \vec{b}$ $= a^0 b^0 - a^1 b^1 - a^2 b^2 - a^3 b^3$	$a \cdot b = a^+ b^- + a^- b^+ - \vec{a}_\perp \cdot \vec{b}_\perp$ $= a^+ b^- + a^- b^+ - a^1 b^1 - a^2 b^2$
Lagrangian density	
$\mathcal{L} = \frac{1}{2} (\partial_0 \phi)^2 - \frac{1}{2} (\vec{\nabla} \phi)^2 - V(\phi)$	$\mathcal{L} = \partial_+ \phi \partial_- \phi - \frac{1}{2} (\vec{\nabla}_\perp \phi)^2 - V(\phi)$
conjugate momenta	
$\pi = \frac{\delta \mathcal{L}}{\delta \partial_0 \phi} = \partial_0 \phi$	$\pi = \frac{\delta \mathcal{L}}{\delta \partial_+ \phi} = \partial_- \phi$
canonical commutation relations	
$[\pi(\vec{x}, t), \phi(\vec{y}, t)]$ $= -i \delta^3(\vec{x} - \vec{y})$	$[\pi(x^-, x_\perp, x^+), \phi(y^-, y_\perp, x^+)]$ $= -\frac{i}{2} \delta(x^- - y^-) \delta^2(\vec{x}_\perp - \vec{y}_\perp)$
Hamilton operator	
$P^0 = \int d^3 x \mathcal{H}(\phi, \pi)$ $\mathcal{H} = \pi \partial_0 \phi - \mathcal{L}$	$P_+ = \int dx^- \int d^2 x_\perp \mathcal{H}(\phi, \pi)$ $\mathcal{H} = \pi \partial_+ \phi - \mathcal{L}$
momentum operator	
$\vec{P} = \int d^3 x \pi \vec{\nabla} \phi$	$P_- = \int dx^- d^2 x_\perp \pi \partial_- \phi$ $\vec{P}_\perp = \int dx^- d^2 x_\perp \pi \vec{\partial}_\perp \phi$
eigenvalue equation	
$P^0 \psi_n\rangle = E_n \psi_n\rangle$ \vec{P} fixed	$P_+ \psi_n\rangle = P_{+n} \psi_n\rangle$ P_-, \vec{P}_\perp fixed
hadron masses	
$M_n^2 = E_n^2 - \vec{P}^2$	$M_n^2 = 2 P_{+n} P_- - \vec{P}_\perp^2$

Table 1: canonical quantization in ordinary coordinates and on the light-front

space sector are used as variational parameters. They are determined by making the expectation value of the energy stationary with respect to variations in the wavefunction. Typically the variation is done for fixed momentum.^{*h*} This whole procedure results in coupled integral equations for the Fock space components. In general they have to be solved numerically. In practical calculations, since one cannot include infinitely many Fock components, one has to introduce some *ad hoc* cutoff in the Fock space. Thus it is very important to demonstrate that physical observables do not depend on how many Fock components are included.

Until one selects the canonically conjugate momenta and postulates equal τ commutation relations, i.e. at the level of the classical Lagrangian, the transition from ET to the LF consists of a mere rewriting. After quantization, the independent degrees of freedom are the fields and their conjugate momenta on the initial surface ($x^0 = 0$ for ET and $x^+ = 0$ for LF). Thus different degrees of freedom are employed to expand physical states in the ET and in the LF approach. Of course, after solving the equations of motion, physical observables must not depend on the choice of quantization plane. However, it may turn out that one approach is more efficient (e.g. faster numerical convergence) than the other or more elegant and more easy to interpret physically. This is particularly the case if one is mostly interested in observables which are dominated by correlation functions in a light-like direction, such as parton distributions, which are much more easily accessible on the LF than in usual coordinates.

3 A First Look at the Light-Front Vacuum

In the Fock space expansion one starts from the vacuum as the ground state and constructs physical hadrons by successive application of creation operators. In an interacting theory the vacuum is in general an extremely complicated state and not known a priori. Thus, in general, a Fock space expansion is not practical because one does not know the physical vacuum (i.e. the ground state of the Hamiltonian). In normal coordinates, particularly in the Hamiltonian formulation, this is a serious obstacle for numerical calculations. As is illustrated in Table 2, the LF formulation provides a dramatic simplification at this point. While all components of the momentum in normal coordinates can be positive as well as negative, the longitudinal LF momentum P_- is always positive. In free field theory (in normal coordinates as well as on the LF) the vacuum is the state which is annihilated by all annihilation operators a_k . In

^{*h*}On the LF this is very important because $P_+ \propto 1/P_-$, i.e. unrestricted variation (P_- allowed to vary) results in $P_- \rightarrow \infty$.

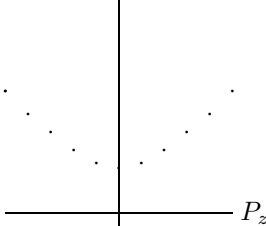
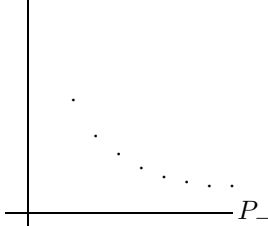
normal coordinates	light-front
free theory	
$P^0 = \sqrt{m^2 + \vec{P}^2}$ 	$P_+ = \frac{m^2 + \vec{P}_\perp^2}{2P_-}$ 
vacuum (free theory)	
$P^0 = \sum_{\vec{k}} a_{\vec{k}}^\dagger a_{\vec{k}} \sqrt{m^2 + \vec{k}^2}$	$P_+ = \sum_{k_-, \vec{k}_\perp} a_{k_-, \vec{k}_\perp}^\dagger a_{k_-, \vec{k}_\perp} \frac{m^2 + \vec{k}_\perp^2}{2k_-}$
vacuum (interacting theory)	
$a_{\vec{k}} 0\rangle = 0$	$a_{k_-, k_\perp} 0\rangle = 0$
<p>many states with $\vec{P} = 0$ (e. g. $a_{\vec{k}}^\dagger a_{-\vec{k}}^\dagger 0\rangle$)</p>	<p>$k_- \geq 0$ \hookrightarrow only pure zero-mode excitations have $P_- = 0$</p>
$\hookrightarrow \tilde{0}\rangle$ very complex	$\hookrightarrow \tilde{0}\rangle$ can only contain zero-mode excitations

Table 2: Zero Modes and the Vacuum

general, in an interacting theory, excited states (excited with respect to the free Hamiltonian) mix with the trivial vacuum (i.e. the free field theory vacuum) state resulting in a complicated physical vacuum. Of course, there are certain selection rules and only states with the same quantum numbers as the trivial vacuum can mix with this state; for example, states with the same momentum as the free vacuum ($\vec{P} = 0$ in normal coordinates, $P_- = 0$, $\vec{P}_\perp = 0$ on the LF). In normal coordinates this has no deep consequences because there are many excited states which have zero momentum. On the LF the situation is completely different. Except for pure zero-mode excitations, i.e. states where only the zero-mode (the mode with $k_- = 0$) is excited, all excited states have positive longitudinal momentum P_- . Thus only these pure zero-mode excitations can mix with the trivial LF vacuum. Thus with the exception of the zero-modes the physical LF vacuum (i.e. the ground state) of an interacting field theory must be trivial (the only exceptions are pathological cases, where the LF Hamiltonian is unbounded from below).

Of course, this cannot mean that the vacuum is entirely trivial. Otherwise it seems impossible to describe many interesting problems which are related to spontaneous symmetry breaking within the LF formalism. For example one knows that chiral symmetry is spontaneously broken in QCD and that this is responsible for the relatively small mass of the pions — which play an important role in strong interaction phenomena at low energies. What it means is that one has reduced the problem of finding the LF vacuum to the problem of understanding the dynamics of these zero-modes.

First this sounds just like merely shifting the problem about the structure of the vacuum from nonzero-modes to zero-modes. However, as the free dispersion relation on the LF,

$$k_+ = \frac{m^2 + \vec{k}_\perp^2}{2k_-}, \quad (6)$$

indicates, zero-modes are high energy modes! Hence it should, at least in principle, be possible to eliminate these zero-modes systematically giving rise to an effective LF field theory.

4 Effective Light-Front Hamiltonians

Above discussion shows that it is clearly wrong to leave out zero-modes degrees of freedom in the sense of just dropping them since this always yields a trivial vacuum. However, this should be distinguished from leaving out zero-modes in the sense of integrating them out. In the second approach the vacuum can be nontrivial, but the nontrivial vacuum structure has been shifted from

the states to the operators. In particular, LF Hamiltonians will in general have to be modified from their canonical form. That this task can actually be accomplished will be illustrated in the following examples.

4.1 The 't Hooft Model

The first model that we will discuss is 1+1 dimensional QCD for an infinite number of colors (the 't Hooft model). The model was first solved by 't Hooft in Ref. ⁶, using naive LF formulation, i.e. starting from the canonical LF Hamiltonian and without zero-modes. Nevertheless, 't Hooft's spectrum was later confirmed by a calculation which employed canonical equal time quantization ⁷. This result is at first very surprising when one considers the fact that the equal time quantized result yielded a nonzero chiral condensate for vanishing quark mass $m_q \rightarrow 0$, while the LF-vacuum was trivial for any value of m_q . a direct evaluation gave of course zero on the LF. However, application of current algebra techniques to meson masses and coupling constants determined by solving the (zero-mode free) LF equations gives a nonzero result for the condensate — even in the zero quark mass limit:

$$\begin{aligned} 0 &= \lim_{q \rightarrow 0} i q^\mu \int d^2 x e^{i q x} \langle 0 | T [\bar{\psi} \gamma_\mu \gamma_5 \psi(x) \bar{\psi} i \gamma_5 \psi(0)] | 0 \rangle \\ &= -\langle 0 | \bar{\psi} \psi | 0 \rangle - 2 m_q \int d^2 x \langle 0 | T [\bar{\psi} i \gamma_5 \psi(x) \bar{\psi} i \gamma_5 \psi(0)] | 0 \rangle. \end{aligned} \quad (7)$$

Upon inserting a complete set of meson states ⁱ one thus obtains

$$\langle 0 | \bar{\psi} \psi | 0 \rangle = -m_q \sum_n \frac{f_P^2(n)}{M_n^2}, \quad (8)$$

where

$$f_P(n) \equiv \langle 0 | \bar{\psi} i \gamma_5 \psi | n \rangle = \sqrt{\frac{N_C}{\pi}} \frac{m_q}{2} \int_0^1 dx \frac{1}{x(1-x)} \phi_n(x) \quad (9)$$

and the wave functions ϕ_n and invariant masses M_n^2 are obtained from solving 't Hooft's bound state equation for mesons in QCD_{1+1}

$$M_n^2 \phi_n(x) = \frac{m_q^2}{x(1-x)} \phi_n(x) + G^2 \int_0^1 dy \frac{\phi_n(x) - \phi_n(y)}{(x-y)^2}. \quad (10)$$

The result for $\langle 0 | \bar{\psi} \psi | 0 \rangle$ obtained this way agrees with the ET calculation ^{8 j}.

ⁱ Because we are working at leading order in $1/N_C$, the sum over one meson states saturates the operator product in Eq.(7).

^j It should be emphasized that the LF calculation preceded the ET calculation.

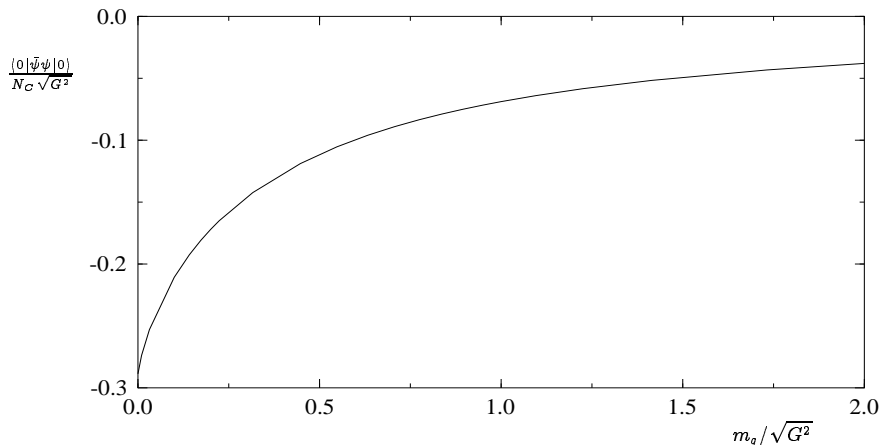


Figure 3: Chiral condensate obtained by evaluating Eq. (8) as a function of the quark mass. For nonzero quark mass, the (infinite) free part has been subtracted. The result agrees for all quark mass with the calculation done using equal time quantization.

This seemingly paradoxical result (peaceful coexistence of a Fock vacuum and a nonzero fermion condensate) can be understood by defining LF quantization through a limiting procedure⁹, where the quantization surface is kept space-like, but being carefully “rotated” to the LF^k. Not all physical quantities behave continuously under this procedure as the LF is approached. For example, the chiral condensate $\langle 0|\bar{\psi}\psi|0\rangle$ has a discontinuous LF limit. On the other hand, the equation of motion for mesons in QCD_{1+1} does have a smooth LF limit. This result explains why the current algebra relation gives the right result for the condensate, even though $\langle 0|\bar{\psi}\psi|0\rangle$ vanishes when evaluated directly on the LF: Since the bound state equation for mesons has a smooth LF limit, both meson masses and coupling constant can be evaluated directly on the LF. Since the current algebra relation (7) is a frame independent relation, it can then be used to extract the condensate from the LF calculation. However, since $\langle 0|\bar{\psi}\psi|0\rangle$ has a discontinuous LF limit, it would be misleading to draw conclusions about the vacuum structure from its value obtained directly on the LF.

Unfortunately, the ’t Hooft model is rather untypical because the effective (in the sense of zero-modes integrated out) LF Hamiltonian for this model is identical to the canonical Hamiltonian, i.e. the naive calculation yielded

^kAnother way of thinking about this procedure is to imagine a gradual boost to infinite momentum.

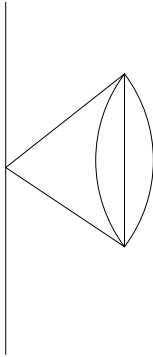


Figure 4: Generalized tadpole (Feynman-) diagram in ϕ^4 theory.

already the correct spectrum. In general, the situation is more complex as we will illustrate in the following examples.

4.2 Self-Interacting Scalar Fields

The most simple example with a non-trivial effective LF Hamiltonian are self-interacting scalar fields described by a Lagrangian of the form

$$\mathcal{L} = \frac{1}{2} \partial_\mu \phi \partial^\mu \phi - \sum_{n=2}^N \frac{\lambda_n}{n!} \phi^n. \quad (11)$$

We will not restrict the dimensionality of space, but, depending on the number of space time dimensions, we will limit the largest power N appearing in the interactions in order to ensure renormalizability. Furthermore, we will implicitly assume that whenever cutoffs are used, compatible cutoffs are used in the LF and ET frameworks, i.e. for example dimensional regularization in the \perp direction or a \perp momentum cutoff.

The main difference between the LF formulation and the ET formulation is that generalized tadpoles (a typical example is shown in Fig.4), i.e. Feynman diagrams where one piece of the diagram is connected to the rest of the diagram only at one point, cannot be generated by a LF Hamiltonian: in time ordered perturbation theory, at least one of the vertices in a generalized tadpole diagram has all lines coming out of or disappearing into the vacuum (Fig.5) — which is forbidden on the LF (without zero-modes).

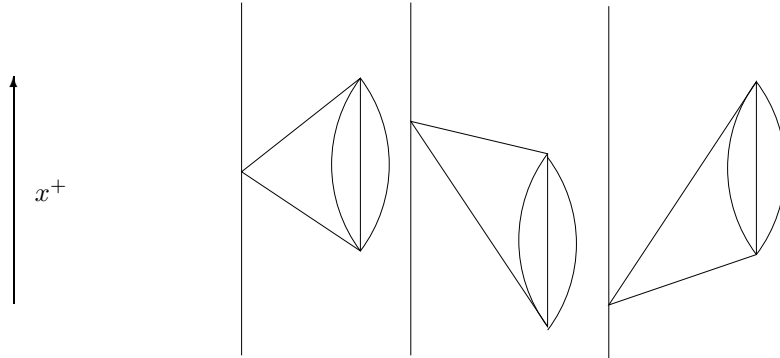


Figure 5: Same as Fig. 4 but as LF-time ordered diagrams. At least one of the vertices has all lines popping out of or disappearing into the vacuum.

So the bad news is that all generalized tadpole diagrams are zero on the LF and they are nonzero in ET quantization, i.e. there is a difference between the perturbation series generated by the two formulations^{10,11}.

The good news is that in self-interacting scalar theories, it is only in generalized tadpole diagrams where such a difference occurs.^l Since generalized tadpoles are only constants, their absence can be compensated for by local counter-terms in the interaction. Note that generalized tadpoles renormalize only ϕ^n -couplings with $n < N$, where N is the largest power appearing in the interaction.

From the purely practical point of view, the difference between LF quantization and ET quantization arises only if one compares calculations done with the same bare parameters! Suppose one would start with parameters that have been chosen so that the bare parameters on the LF include already the counter-terms that are necessary to compensate for the absence of tadpoles. Then ET and LF formulation should give the same results for all n-point Green's functions, i.e. physical observables should be the same. But how can one find the appropriate counter-terms without having to refer to an ET calculation? There is nothing easier than that: simply by using only physical input parameters to fix the bare parameters! For example, if one matches the physical masses of a few particles between an ET calculation and a LF calculation then the bare parameters that one needs in order to get these masses will be different in ET and LF quantization. The difference will be just such that it compensates for

^lTo my knowledge, there is no strict proof of this result, but it is based on handwaving arguments as well as on a thorough three loop analysis.

the absence of tadpoles on the LF and hence all further observables will be the same. In other words there is no problem at all with the LF formulation — despite the absence of all generalized tadpole diagrams. The only situation where one needs to be a little careful in the LF approach is a situation where spontaneous symmetry breaking occurs in the ET formulation. In this case, one has to allow for odd terms in ϕ in the effective LF Hamiltonian, while the ET Hamiltonian contains only even terms.

Beyond this happy ending, there is one more very interesting aspect to this story, which has to do with vacuum condensates. For example, every generalized tadpole diagram in ϕ^4 theory is numerically equal to a diagram that contributes to $\langle 0|\phi^2|0\rangle$. For example, the tadpole in Fig. 4 is proportional to a term that contributes to $\langle 0|\phi^2|0\rangle$ to second order in λ . In fact, after working out the details one finds that the additional LF counter-term, necessary to obtain equivalence between ET and LF quantization is a mass counter-term¹¹

$$\Delta m^2 = \lambda \langle 0 | \frac{\phi^2}{2} | 0 \rangle, \quad (12)$$

where λ is the four point coupling and the vacuum expectation value (VEV) on the r.h.s. is to be evaluated in normal coordinates.

This result can be readily generalized to an arbitrary polynomial interaction. One finds the following dictionary: perturbation theory based on a canonical equal time Hamiltonian with

$$\mathcal{L}_{int}^{ET} = \sum_n \lambda_n \frac{\phi^n}{n!} \quad (13)$$

and perturbation theory based on a canonical light-front Hamiltonian with

$$\mathcal{L}_{int}^{LF} = \sum_n \tilde{\lambda}_n \frac{\phi^n}{n!} \quad (14)$$

are equivalent if

$$\tilde{\lambda}_n = \sum_{k \leq n} \lambda_{n-k} \langle 0 | \frac{\phi^k}{k!} | 0 \rangle. \quad (15)$$

In Ref.¹¹ this fundamental result was derived perturbatively and the prescription for constructing the effective Hamiltonian was tested non-perturbatively by calculating physical masses of excited “mesons” and solitons in the sine-Gordon model.

It is very tempting to conjecture that this dictionary (15) also holds for non-perturbative condensates (such as condensates which arise after spontaneous symmetry breaking). While a general proof is still missing, it has indeed

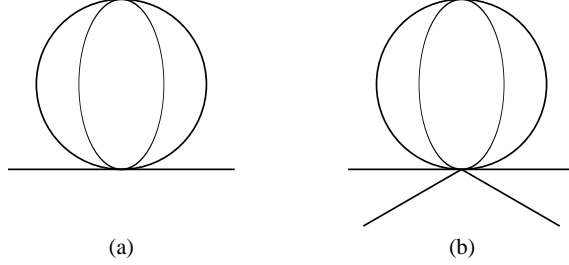


Figure 6: Generalized tadpole diagrams for scalar field theories with higher polynomial interactions. Both are set to zero in LF quantization without zero-modes. Both are proportional to $\langle 0|\phi^4|0\rangle$. The diagram in a.) gives rise to a mass renormalization counter-term and b.) renormalizes the four-point interaction.

been possible to demonstrate for a few specific models that the conjecture is correct¹².

It should also be emphasized that these equivalence considerations hold irrespective of the number of space-time dimensions, i.e. they apply to 1+1 as well as 2+1 and 3+1 dimensional theories. One must only be careful to use commensurate cutoffs when comparing ET and LF quantized theories. An example would be a transverse lattice cutoff, which can be employed both in ET quantization as well as in LF quantization.

What makes all these results particularly interesting is that the effective (zero-modes integrated out) couplings in the effective LF-Hamiltonians contain condensates which shows how non-perturbative effects can “sneak” into the LF formalism and how one can resolve the apparent conflict between trivial LF vacua and nontrivial vacuum effects.

4.3 Fermions with Yukawa Interactions

Eventually, we are interested to understand chiral symmetry breaking in QCD, i.e. we need to understand fermions. As a first step in this direction let us consider a Yukawa model in 1+1 dimensions

$$\mathcal{L} = \bar{\psi} (i \not{\partial} - m_F - g\phi\gamma_5) \psi - \frac{1}{2}\phi (\square + m_B^2) \phi. \quad (16)$$

The main difference between scalar and Dirac fields in the LF formulation is that not all components of the Dirac field are dynamical: multiplying the Dirac equation

$$(i \not{\partial} - m_F - g\phi\gamma_5) \psi = 0 \quad (17)$$

by $\frac{1}{2}\gamma^+$ yields a constraint equation (i.e. an “equation of motion” without a time derivative)

$$i\partial_- \psi_{(-)} = (m_F + g\phi\gamma_5) \gamma^+ \psi_{(+)}, \quad (18)$$

where

$$\psi_{\pm} \equiv \frac{1}{2} \gamma^{\mp} \gamma^{\pm} \psi. \quad (19)$$

For the quantization procedure, it is convenient to eliminate $\psi_{(-)}$, using

$$\psi_{(-)} = \frac{\gamma^+}{2i\partial_-} (m_F + g\phi\gamma_5) \psi_{(+)} \quad (20)$$

from the classical Lagrangian before imposing quantization conditions, yielding

$$\begin{aligned} \mathcal{L} = & \sqrt{2} \psi_{(+)}^{\dagger} \partial_+ \psi_{(+)} - \phi (\square + m_B^2) \phi - \psi_{(+)}^{\dagger} \frac{m_F^2}{\sqrt{2}i\partial_-} \psi_{(+)} \\ & - \psi_{(+)}^{\dagger} \left(g\phi \frac{m_F\gamma_5}{\sqrt{2}i\partial_-} + \frac{m_F\gamma_5}{\sqrt{2}i\partial_-} g\phi \right) \psi_{(+)} - \psi_{(+)}^{\dagger} g\phi \frac{1}{\sqrt{2}i\partial_-} g\phi \psi_{(+)}. \end{aligned} \quad (21)$$

The rest of the quantization procedure very much resembles the procedure for self-interacting scalar fields. In particular, one must be careful about generalized tadpoles, which might cause additional counter-terms in the LF Hamiltonian. In the Yukawa model one usually (i.e. in a covariant formulation) does not think about tadpoles. However, after eliminating $\psi_{(-)}$, we are left with a four-point interaction in the Lagrangian, which does give rise to time-ordered diagrams that resemble tadpole diagrams (Fig.7). In fact, the four-point interaction gives rise to diagrams where a fermion emits a boson, which may or may not self-interact, and then re-absorb the boson at the same LF-time.^m As we discussed already in detail in the context of self-interacting scalar fields, such interactions cannot be generated by a LF Hamiltonian, i.e. the LF formalism defines such tadpoles to be zero.

For self-interacting scalar fields, the difference between ET and LF perturbation theory which thus results can be compensated by a redefinition of parameters that appear already in the Lagrangian. In the Yukawa model, the situation is a little more complicated. The missing tadpoles have the same operator/Lorentz structure as the so called kinetic mass term

$$\mathcal{P}_{kin}^- = \psi_{(+)}^{\dagger} \frac{m_F^2}{\sqrt{2}i\partial_-} \psi_{(+)}. \quad (22)$$

^mThere are also tadpoles, where the fermions get contracted. But those only give rise to an additional boson mass counter-term, but not to a non-covariant counter-term that we investigate here.

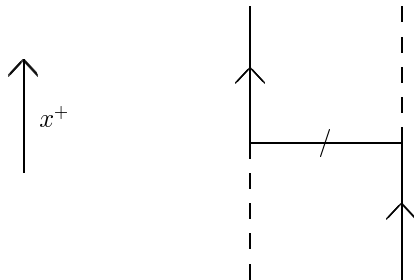


Figure 7: Four point interaction in Yukawa theory that arises after eliminating $\psi_{(-)}$. The crossed out full line represents the instantaneous fermion exchange interaction that results from this elimination. Contracting the boson lines (dashed) yields a diagram analogous to the tadpole diagrams for self-interacting scalar fields.

One obtains this result by contracting the two scalar fields in the four-point interaction. More details can be found in Ref. ¹³. The important point here is that there is no similar counter-term for the term linear in the fermion mass m_F . Thus the difference between ET and LF quantization cannot be compensated by tuning the bare masses differently. The correct procedure requires to renormalize the kinetic mass term (the term $\propto m_F^2$) and the vertex mass term (the term $\propto m$) independent from each other. More explicitly this means that one should make an ansatz for the renormalized LF Hamiltonian density of the form

$$\begin{aligned} \mathcal{P}^- &= \frac{m_B^2}{2} \phi^2 + \psi_{(+)}^\dagger \frac{c_2}{\sqrt{2}i\partial_-} \psi_{(+)} + c_3 \psi_{(+)}^\dagger \left(\phi \frac{\gamma_5}{\sqrt{2}i\partial_-} + \frac{\gamma_5}{\sqrt{2}i\partial_-} g\phi \right) \psi_{(+)} \\ &+ c_4 \psi_{(+)}^\dagger \phi \frac{1}{\sqrt{2}i\partial_-} \phi \psi_{(+)}, \end{aligned} \quad (23)$$

where the c_i do not necessarily satisfy the canonical relation $c_3^2 = c_2 c_4$. However, this does not mean that the c_i are completely independent from each other. In fact, only for specific combinations of c_i will Eq.(23) describe the Yukawa model. It is only that we do not know the relation between the c_i .ⁿ

Thus the bad new is that the number of parameters in the LF Hamiltonian has increased by one (compared to the Lagrangian). The good news is that a wrong combination of c_i will in general give rise to a parity violating

ⁿIt is conceivable that coupling constant coherence ¹⁴ might also be helpful in finding the “unknown relation”, but I have not been able to figure out how to use this idea in the context of a superrenormalizable model such as above model.

theory.^o This is good news because one can thus use parity invariance for physical observables as an additional renormalization condition to determine the additional “free” parameter.

In fact, in Ref.¹⁵, it was shown that utilizing parity constraints as non-perturbative renormalization conditions is practical. The observable considered in that work was the vector transition form factor (in a scalar Yukawa theory in 1+1 dimensions) between physical meson states of opposite C-parity (and thus supposedly opposite parity)

$$\langle p', n | j^\mu | p, m \rangle \stackrel{!}{=} \varepsilon^{\mu\nu} q_\nu F_{mn}(q^2), \quad (24)$$

where $q = p' - p$. When writing the r.h.s. in terms of one invariant form factor, use was made of both vector current conservation and parity invariance. A term proportional to $p^\mu + p'^\mu$ would also satisfy current conservation, but has the wrong parity. A term proportional to $\varepsilon^{\mu\nu} (p_\nu + p'_\nu)$ has the right parity, but is not conserved and a term proportional to q^μ is both not conserved and violates parity. Other vectors do not exist for this example. The Lorentz structure in Eq. (24) has nontrivial implications even if we consider only the “good” component of the vector current^p, yielding

$$\frac{1}{q^+} \langle p', n | j^+ | p, m \rangle = F_{mn}(q^2). \quad (25)$$

That this equation implies nontrivial constraints can be seen as follows: as a function of the longitudinal momentum transfer fraction $x \equiv q^+/p^+$, the invariant momentum transfer reads (M_m^2 and M_n^2 are the invariant masses of the in and outgoing meson)

$$q^2 = x \left(M_m^2 - \frac{M_n^2}{1-x} \right) \quad (26)$$

Typically, there are two values of x that lead to the same value of q^2 . It is

^oAs an example, consider the free theory, where the correct relation ($c_3^2 = c_2 c_4$) follows from a covariant Lagrangian. Any deviation from this relation can be described on the level of the Lagrangian (for free massive fields, equivalence between LF and covariant formulation is not an issue) by addition of a term of the form $\delta\mathcal{L} = \bar{\psi} \frac{\gamma^+}{i\partial^+} \psi$, which is obviously parity violating, since parity transformations result in $A^\pm \rightarrow A^\mp$ for Lorentz vectors A^μ ; i.e. $\delta\mathcal{L} \rightarrow \bar{\psi} \frac{\gamma^-}{i\partial^-} \psi \neq \delta\mathcal{L}$.

^pIn the context of LF calculations, currents that are bilinear in the dynamical component $\psi_{(+)}$ are usually easiest to renormalize and calculate. Other combinations, such as $\psi_{(-)}^\dagger \psi_{(-)}$ involve interactions when expressed in terms of the dynamical components and are thus terrible to handle — hence they are often referred to as “bad” components.

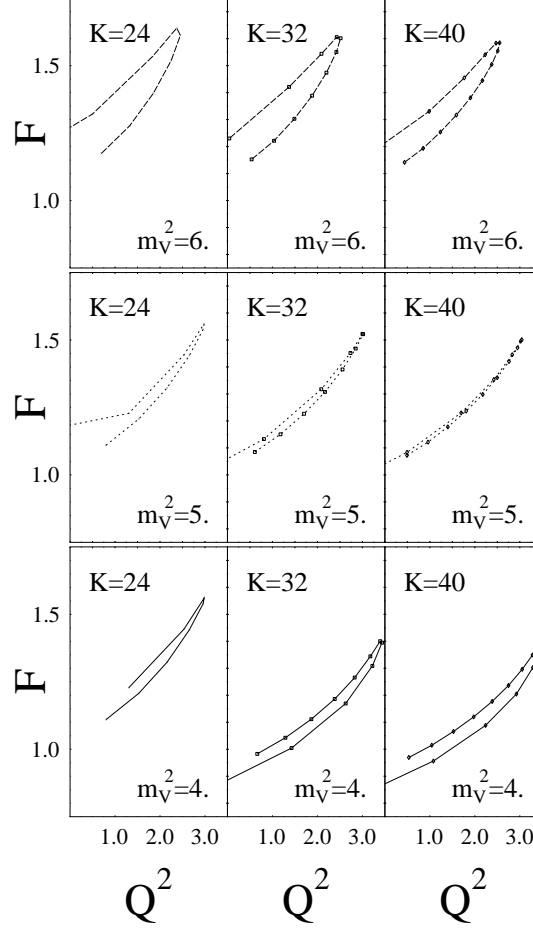


Figure 8: Inelastic transition form factor (25) between the two lightest meson states of the Yukawa model, calculated for various vertex masses m_v and for various DLCQ parameters K . The physical masses for the fermion and the scalar meson have been renormalized to the values $(m_F^{phys})^2 = (m_S^{phys})^2 = 4$. All masses and momenta are in units of $\sqrt{\lambda} = \sqrt{c_4/2\pi}$. In this example, only for $m_V^2 \approx 5$ one obtains a form factor that is a unique function of Q^2 , i.e. only for $m_V^2 \approx 5$, the result is consistent with Eq. (25). Therefore, only for this particular value of the vertex mass, is the matrix element of the current operator consistent with both parity and current conservation.

highly nontrivial to obtain the same form factor for both values of x . In Ref. ¹⁵, the coupling as well as the physical masses of both the fermion and the lightest boson were kept fixed, while the “vertex mass” was tuned (note that this required re-adjusting the bare kinetic masses). Figure 8 shows a typical example. In that example, the calculation of the form factor was repeated for three values of the DLCQ parameter K (24, 32 and 40) in order to make sure that numerical approximations did not introduce parity violating artifacts.

For the “magic value” of the vertex mass one finds that the parity condition (25) is satisfied over the whole range of q^2 considered. This provides a strong self-consistency check, since there is only one free parameter, but the parity condition is not just one condition but a condition for every single value of q^2 (i.e. an infinite number of conditions). In other words, keeping the vertex mass independent from the kinetic mass is not only necessary, but also seems sufficient in order to properly renormalize Yukawa_{1+1} .

However, note that, depending on the cutoff used, the kinetic mass counter-term may or may not be a function of the momenta¹⁷. If one uses a cutoff which breaks manifest boost invariance, such as a DLCQ cutoff, then the kinetic mass counter-term will in general have to be a function of the longitudinal momenta. On the other hand, if one uses cutoffs which preserve manifest boost invariance, such as cutoffs on ratios of momenta or invariant mass transfers at each vertex then the kinetic mass counter-term can be taken to be momentum independent and thus counter-term functions can be avoided in this model.

It is still an open question whether “counter-term functions”¹⁹ can be avoided in general, i.e. in 3+1 dimensions. In non-gauge theories, preliminary investigations (see also Section 4.4 suggest that counter-term functions can be avoided if one uses a cutoff where longitudinal and transverse momenta are cut off independently and the cutoff must at the same time be manifestly boost invariant in the longitudinal direction. For gauge theories, the same condition seems to hold, except that the transverse momenta must be cut off in a gauge invariant way (to avoid disastrous longitudinal divergences) by using dimensional regularization or a transverse lattice.

4.4 A 3+1 Dimensional Model with Spontaneous Chiral Symmetry Breaking

One would like to study a 3+1 dimensional model which goes beyond the mean field approximation (NJL !), but on the other hand being too ambitious results in very difficult or unsolvable models.⁹ We decided to place the following constraints on our model:¹⁸

⁹For example, demanding Lorentz invariance, chiral symmetry and asymptotic freedom leaves QCD as the most simple model.

- Most importantly, the model should be 3+1 dimensional, but we do not require full rotational invariance.
- The model should have spontaneous χ SB (but not just mean field)
- Finally, it should be solvable both on the LF and using a conventional technique (to provide a reference calculation).

Given these constraints, the most simple model that we found is described by the Lagrangian

$$\mathcal{L} = \bar{\psi}_k \left[\delta^{kl} (i\not{\partial} - m) - \frac{g}{\sqrt{N_c}} \vec{\gamma}_\perp \vec{A}_\perp^{kl} \right] \psi_l - \frac{1}{2} \vec{A}_\perp^{kl} (\square + \lambda^2) \vec{A}_\perp^{kl}, \quad (27)$$

where k, l are “color” indices ($N_c \rightarrow \infty$), $\perp = x, y$ and where a cutoff is imposed on the transverse momenta. A fermion mass was introduced to avoid pathologies associated with the strict $m = 0$ case. χ SB can be studied by considering the $m \rightarrow 0$ limit of the model.

The reasons for this bizarre choice of model [Eq. (27)] are as follows. If one wants to study spontaneous breaking of chiral symmetry, then one needs to have a chirally invariant interaction to start with, which motivates a vector coupling between fermions and bosons. However, we restricted the vector coupling to the \perp component of a vector field since otherwise one has to deal with couplings to the “bad” current $j^-{}^r$. In a gauge theory, such couplings can be avoided by choice of gauge, but we preferred not to work with a gauge theory, since this would give rise to additional complications from infrared divergences. Furthermore, we used a model with “color” degrees of freedom and considered the limit where the number of colors is infinite, because such a model is solvable, both on and off the LF. No interaction among the bosons was included because this would complicate the model too much. Finally, we used a cutoff on the transverse momenta because such a cutoff can be used both on the LF as well as in normal coordinates and therefore one can compare results from these two frameworks already for finite values of the cutoff.

Because we are considering the limit $N_c \rightarrow \infty$, of Eq. (27), the iterated rainbow approximation for the fermion self-energy Σ becomes exact, which we used to solve the model in the Dyson-Schwinger approach. On the one hand this provides a reference calculation, but one can also use the solution to show that for sufficiently large coupling constant, the physical mass for the fermion remains finite in the limit $m \rightarrow 0$, proving the spontaneous breakdown of chiral symmetry in the model.

^r j^- is bilinear in the constrained component of the fermion field, which makes it very difficult to renormalize this component of the current in the LF framework.

Since we wanted to investigate the applicability of the effective LF Hamiltonian formalism, we formulated above model on the LF without explicit zero-mode degrees of freedom. The bottom line of this investigation was as follows (for details see Ref. ¹⁸).

- The LF Green's function equation and the DS equation are identical (and thus have identical solutions) if and only if one introduces an additional (in addition to the self-induced inertias) counter-term to the kinetic mass term for the fermion.
- For fixed transverse momentum cutoff, this additional kinetic mass term is finite.
- The value of the vertex mass in the LF Hamiltonian is the same as the value of the current mass in the DS equation.
- In the chiral limit, mass generation for the (physical) fermion occurs through the kinetic mass counter term
- The effective interaction (after integrating out 0-modes) can be summarized by a few simple terms — which are already present in the canonical Hamiltonian.

Even though we determined the kinetic mass counter term by directly comparing the LF and DS calculation, several methods are conceivable which avoid reference to a non-LF calculation in order to set up the LF problem. One possible procedure would be to impose parity invariance for physical observables as a constraint ¹⁵.

5 Dynamical Vertex Mass Generation and Chiral Symmetry Breaking on the LF

Naively, helicity flip amplitudes for fermions seem to vanish in the chiral limit of light-front QCD, which would make it nearly impossible to generate a small pion mass in this framework. In this Section, a simple model is used to illustrate how a large helicity flip amplitude is generated dynamically by summing over an infinite number of Fock space components. Implications for the renormalization of light-front Hamiltonians for fermions are discussed.

In the LF-formulation, only half of the spinor components are dynamical degrees of freedom in the sense that their equation of motion involves a time derivative. Upon introducing $\psi_{(\pm)} = \gamma^{\pm} \gamma^{\mp} \psi / 2$, one finds for example in QCD

that $\psi_{(-)}$ satisfies a constraint equation¹⁹

$$i\partial_{-}\psi_{(-)} = \left[\vec{\alpha}_{\perp} \cdot \left(i\vec{\partial}_{\perp} + g\vec{A}_{\perp} \right) + \gamma^0 m_F \right] \psi_{(+)} \quad (28)$$

and $\psi_{(-)}$ is usually eliminated (using this constraint equation) from the Lagrangian before quantizing the theory. Thus the Hamiltonian contains both a term quadratic in the fermion mass (the kinetic energy term for the fermions) and one term which is linear in the fermion mass (one gluon vertex with helicity flip).

It has been known for a long time that integrating out zero-mode degrees of freedom results in a nontrivial renormalization of the quadratic (kinetic!) mass term²⁰ but the linear (helicity flip vertex!) mass term in the Hamiltonian is unaffected by strict zero modes and the “vertex mass” must be identified with the current quark mass which vanishes in the chiral limit (see the previous section as well as Refs: ^{19,18,21}).

It is very easy to see how a constituent quark picture can emerge in such an approach. However, it always seemed mysterious how one can obtain a massless π meson in such a picture without having at the same time a massless ρ : when the helicity flip term for quarks is omitted, π and ρ become partners in a degenerate multiplet²¹. The key observation to resolve this problem is that one needs to find a mechanism which dynamically generates a large helicity flip amplitude. At first this seems impossible since every LF-time ordered diagram (any order in the coupling!) which flips the helicity of the fermion contains at least one power of the vertex mass (which vanishes in the chiral limit).

Above argument does not rule out the possibility that summing over an infinite class of time-ordered diagrams (including an infinite number of Fock space components) can lead to divergences which can compensate for the suppression of individual diagrams. A simple model to illustrate this idea is a fermion field with (fundamental) “color” degrees of freedom coupled to the transverse components of a massive vector field (adjoint representation)

$$\mathcal{L} = \bar{\psi} \left(i\partial_{-} - m - \frac{g}{\sqrt{N_C}} \vec{\gamma}_{\perp} \vec{A}_{\perp} \right) \psi - \frac{1}{2} \text{tr} \left(\vec{A}_{\perp} \square \vec{A}_{\perp} + \lambda^2 \vec{A}_{\perp}^2 \right). \quad (29)$$

We will take the limit $N_C \rightarrow \infty$, where the planar approximation becomes exact. Furthermore, we will assume that the fields depend on longitudinal coordinates only, i.e. we consider a dimensionally reduced version of the model. Because of the $N_C \rightarrow \infty$ limit, the model still has spontaneous breaking of chiral symmetry as $m \rightarrow 0$. This can be shown by solving the covariant self-

energy equation

$$\Sigma(p) = g^2 \int \frac{d^2 k}{(2\pi^2)} \vec{\gamma}_\perp \frac{1}{\not{k} - m - \Sigma(k)} \vec{\gamma}_\perp \frac{1}{(p-k)^2 - \lambda^2} \quad (30)$$

self-consistently. Note that Σ becomes effectively momentum independent for $\lambda \rightarrow \infty$, yielding a simplified gap equation

$$M = m + M \frac{g^2 M}{2\pi\lambda^2} \ln \frac{\lambda^2}{M^2}, \quad (31)$$

where M is the physical mass of the fermion.

It is easy to see how *dynamical vertex mass generation* emerges in the limit where λ , the mass of the boson, is very large (in order to avoid a trivial theory, the coupling constant is rescaled accordingly). In this limit, self-energies are momentum independent and one can thus absorb all self-energies into a redefinition of the kinetic mass, by setting it equal to the physical mass M , which satisfies the above gap-equation (31), i.e.

$$M = \frac{m}{1 - \frac{g^2}{2\pi\lambda^2} \ln \frac{\lambda^2}{M^2}}. \quad (32)$$

However, this does not yet explain how a large helicity flip amplitude emerges. For this purpose, let us consider a helicity flip process and focus on all those diagrams which are linear in the vertex mass, i.e. contain only one helicity flip vertex. After redefining the kinetic mass as the physical mass, we should no longer take diagrams with self-mass sub-diagrams^s into account since this would amount to double counting. Without self-mass sub-diagrams and in the planar approximation considered here, this leaves only a very simple class of diagrams which are linear in the vertex mass. In the following, we will study this class in detail and sum it up to all orders in perturbation theory.

First of all, since we work in a dimensionally reduced model, boson-fermion vertices are linear in the vertex mass, unless they are instantaneous vertices, i.e. the limitation to terms linear in the vertex mass means that all but one vertex in a given time ordered diagram must be instantaneous. This means that, to leading order in the vertex mass, a general higher order diagram for a helicity flip vertex is obtained by attaching an instantaneous interaction to the external vertex and then another one to the boson line emanating from the first instantaneous vertex and so on until the last boson line ends up in the actual helicity flip vertex. Typical diagrams are depicted in Fig. 9^t Let

^sI.e. sub-diagrams with only two external fermion lines, which are both on mass shell.

^tOf course, in addition to the diagrams in Fig. 9, there are corrections to the helicity flip amplitude on the other side of the external vertex, but up to kinematical factors, they are identical to the ones depicted in Fig. 9.

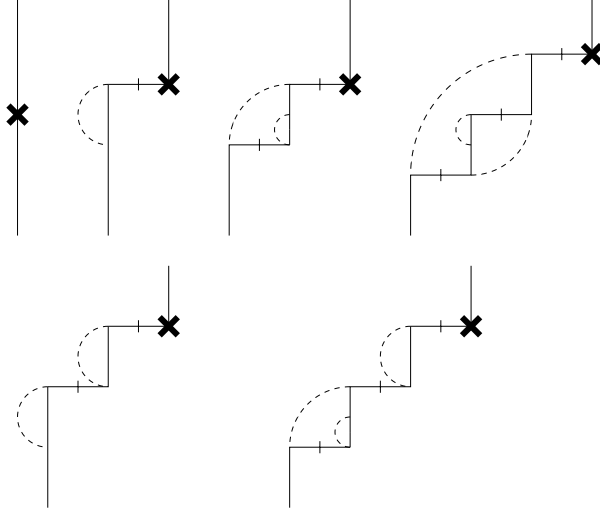


Figure 9: LF-time ordered diagrams contributing to the helicity flip amplitude for a fermion. The external vertex is depicted as a cross. The dashed lines are boson fields and the slashed lines represent LF-instantaneous interactions. In the limit of a heavy boson mass, the diagrams in the top row dominate.

us first look at the “bare rainbow” diagrams ^u in the top row of Fig. 9. The first diagram is just the bare vertex. The second diagram yields up to overall kinematical factors (Fig.10a)

$$T_{flip}^{2a} = m_V \frac{g^2}{2\pi} I_1, \quad (33)$$

where

$$I_1 = \int_0^1 \frac{dx}{(1-x)} \frac{\frac{1}{x} - 1}{p^2 - \frac{M^2}{x} - \frac{\lambda^2}{1-x}} \xrightarrow{\lambda \rightarrow \infty} \frac{1}{\lambda^2} \ln \frac{\lambda^2}{M^2}. \quad (34)$$

The forth order bare rainbow is a little more complicated, yielding (up to the same overall factors as Eq. (33) (Fig. 10b)

$$T_{flip}^{2b} = g^4 m_V \int_0^1 \frac{dx/(1-x)}{P^2 - \frac{M^2}{x} - \frac{\lambda^2}{1-x}} \frac{1}{x} \int_0^x \frac{dy/(x-y) \left(\frac{1}{y} - \frac{1}{x} \right)}{p^2 - \frac{M^2}{y} - \frac{\lambda^2}{x-y} - \frac{\lambda^2}{1-x}}. \quad (35)$$

^uWe call these diagrams bare rainbow diagrams, since they really have the topology of a rainbow, as distinguished from iterated or nested rainbows.

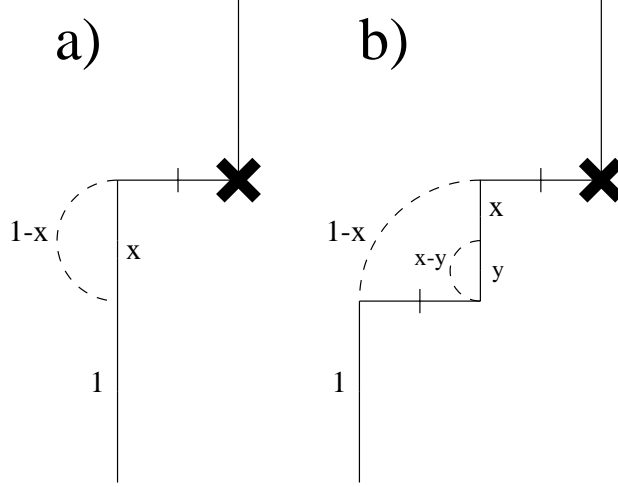


Figure 10: Lowest order bare rainbow diagrams.

The x integral in Eq. (35) is dominated by small values of x as $\lambda \rightarrow \infty$. This allows us to simplify the y integral ($z = y/x$)

$$\begin{aligned} \int_0^x \frac{dy}{x-y} \frac{\left(\frac{1}{y} - \frac{1}{x}\right)}{p^2 - \frac{M^2}{y} - \frac{\lambda^2}{x-y} - \frac{\lambda^2}{1-x}} &= \int_0^1 \frac{dz}{1-z} \frac{\left(\frac{1}{z} - 1\right)}{x \left(p^2 - \frac{\lambda^2}{1-x}\right) - \frac{M^2}{z} - \frac{\lambda^2}{1-z}} \\ &\xrightarrow{x \rightarrow 0} \int_0^1 \frac{dz}{1-z} \frac{\left(\frac{1}{z} - 1\right)}{\frac{M^2}{z} + \frac{\lambda^2}{1-z}} \xrightarrow{\lambda \rightarrow \infty} -I_1, \end{aligned} \quad (36)$$

i.e.

$$T_{flip}^{2b} = m_V \left(\frac{g^2}{2\pi} I_1 \right)^2. \quad (37)$$

It turns out that the bare rainbow diagrams form a geometric series, yielding (together with the bare vertex)

$$T_{flip}^{bare \text{ rainbow}} = \frac{m_V}{1 - \frac{g^2}{2\pi} I_1} = \frac{m_V}{1 - \frac{g^2}{2\pi\lambda^2} \ln \frac{\lambda^2}{M^2}}. \quad (38)$$

Besides the bare rainbow diagrams one also needs to consider the nested rainbow diagrams (bottom row of Fig. 9), where the the direction of the chain of instantaneous interactions does not always alternate along the fermion line.

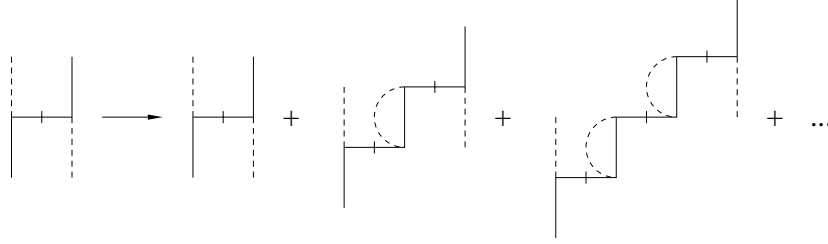


Figure 11: Chain of instantaneous interactions leading to a geometric series.

These can be obtained from the bare rainbow diagrams by replacing each instantaneous interaction by a chain of instantaneous interactions (Fig. 11) leading again to a geometric series as $\lambda \rightarrow \infty$ ^v, which can be incorporated into the above result by making the replacement

$$g^2 \rightarrow \frac{g^2}{1 - \frac{g^2}{2\pi} I_2}, \quad (39)$$

where

$$I_2 = \int_0^1 \frac{dx}{(1-x)} \frac{1}{p^2 - \frac{M^2}{x} - \frac{\lambda^2}{1-x}} \xrightarrow{\lambda \rightarrow \infty} -\frac{1}{\lambda^2} \quad (40)$$

in each instantaneous interaction. Together with Eq. (38), this yields for the sum of all planar helicity flip diagrams in leading order in the vertex mass

$$T_{flip}^{full \text{ rainbow}} = \frac{m_V}{1 - \frac{g^2}{2\pi} \frac{I_1}{1 - \frac{g^2}{2\pi} I_2}}. \quad (41)$$

However, since $I_2/I_1 \sim 1/\ln \lambda^2 \xrightarrow{\lambda \rightarrow \infty} 0$, one can neglect I_2 in Eq. (41), yielding

$$T_{flip}^{full \text{ rainbow}} \xrightarrow{\lambda \rightarrow \infty} \frac{m_V}{1 - \frac{g^2}{2\pi \lambda^2} \ln \frac{\lambda^2}{M^2}}, \quad (42)$$

i.e. just the bare result above (38).

The crucial point is that the denominator of Eq. (42) becomes small in the chiral limit, as one can read off from the gap equation (32). In other words, even though each individual diagram in Fig. (9) vanishes in the chiral limit $\propto m$, summing over an infinite number of diagrams yields $T_{flip} \propto M$, which remains finite as $m \rightarrow 0$.

Several interesting observations can be made from this example:

^vOnly for $\lambda \rightarrow \infty$ can one neglect the energy dependence of these bubbles.

- While integrating out zero-modes contribute significantly to the kinetic mass of fermions, there is no such contribution to the vertex mass from strict zero-modes. However, the vertex mass gets renormalized by (infinitesimally) small x contributions since one has to sum over an infinite number of Fock space components in order to obtain a finite helicity flip amplitude in the chiral limit.
- In realistic non-perturbative calculations of hadron spectra, where one cannot include an infinite number of Fock space components, it will at some level be necessary to absorb the higher order corrections into an effective vertex mass M .
- The leading diagrams (top row in Fig. 9) have a relatively simple structure: higher order diagrams can be successively built by replacing the bare helicity flip vertex inside a given diagram with the second order dressed helicity flip vertex. This observation may be useful for a renormalization group study of the helicity flip interactions, since a large amplitude is obtained only through an infinite chain of steps from finite x down to vanishingly small values of x . Qualitatively, this mechanism resembles the chiral symmetry breaking mechanism suggested in Ref. ²³.

6 Summary

LF coordinates play a distinguished role in many high energy scattering experiments (e.g. DIS) and LF quantization represents the most physical approach towards a fundamental theoretical description of such experiments. Lf quantization also yields the very interesting but also controversial result that LF vacua are trivial. The apparent contradiction between non-trivial vacua in an equal time formulation and trivial vacua on the LF is resolved by introducing effective LF Hamiltonians, where the non-trivial vacuum structure is not “gone” but has been absorbed into effective interaction terms. In a sense, the non-trivial vacuum structure has been shifted from the states to the operators. This result was illustrated by studying QCD_{1+1} , scalar fields (1+1 and 3+1 dimensions), Yukawa theories and a (3+1 dimensional) model with spontaneous breakdown of chiral symmetry. Finally, I illustrated in a model how a large helicity flip amplitude (necessary to produce $\pi - \rho$ or $N - \Delta$ splitting!) emerges in the chiral limit by summing over an infinite number of Fock space components. In a practical numerical calculation (finite number of Fock components), this physics must be put in by hand, i.e. by modifying the Hamiltonian. In the model, this could be accomplished by keeping the vertex mass finite in the chiral limit (dynamical vertex mass generation).

In these lectures, I have presented a number of examples which show that effective LF Hamiltonians, with zero modes integrated out, can indeed give the same physics (e.g. spectrum) as equal time Hamiltonians — despite the fact that the LF-vacuum is trivial, and even in situations where symmetries are spontaneously broken in an equal time framework. These results certainly constitute an important and encouraging step towards formulating LF-QCD. Nevertheless, what is still missing is an understanding of how longitudinal gauge fields and the notorious small k^+ divergences arising in LF gauge fit into above picture.

Acknowledgements

I would like to thank C.R. Ji and D.P. Min for inviting me to give lectures at this interesting summer school. This work was supported by the D.O.E. under contract DE-FG03-96ER40965 and in part by TJNAF.

References

1. M. Burkardt, *Advances Nucl. Phys.* **23**, 1 (1996).
2. P.A.M. Dirac, *Rev. Mod. Phys.* **21**, 392 (1949).
3. S.J. Brodsky, H.-C. Pauli and S.S. Pinsky, *submitted to Phys. Reports*, hep-ph/9705477.
4. J.D. Bjorken and S.D. Drell, “Relativistic Quantum Fields”, (McGraw Hill, New York, 1965).
5. S.-J. Chang, R.G. Root and T.-M. Yan, *Phys. Rev.* **D7** (1972) 1133; S.-J. Chang and T.-M. Yan, *Phys. Rev.* **D7** (1972) 1147.
6. G.’t Hooft, *Nucl. Phys. B* **72** (1974) 461; *ibid.* **B 75** (1974) 461.
7. M. Li, *Phys. Rev. D* **34**, 3888 (1986).
8. A.R. Zhitnitsky, *Phys. Lett. B* **165**, 405 (1985); *Sov. J. Nucl. Phys.* **43**, 999 (1986); *ibid.* **44**, 139 (1986); M. Burkardt, *Phys. Rev. D* **53**, 933 (1996); talk given at “Workshop on Quantum Infrared Physics”, Paris, June 1994, hep-ph/9409333.
9. E.V. Prokhvatilov, V.A. Franke, *Yad. Fiz.* **49**, 1109 (1989); F. Lenz, S. Levit, M. Thies and K. Yazaki, *Ann. Phys.(N.Y.)* **208** (1991) 1; F. Lenz, *Proceedings of NATO Advanced Study Institute on “Hadrons and Hadronic Matter”*, eds. D. Vautherin et al. (Plenum, New York, 1990); K. Hornbostel, *Phys. Rev. D* **45**, 3781 (1992).
10. P.A. Griffin, *Phys. Rev. D* **46**, 3538 (1992).
11. M. Burkardt, *Phys. Rev. D* **47**, 4628 (1993).
12. E.V. Prokhvatilov, H.W.L. Naus and H.-J. Pirner, *Phys. Rev. D* **51**, 2933 (1995).

13. M. Burkardt and A. Langnau, Phys. Rev. D **44**, 3857 (1991).
14. R.J. Perry, invited lectures presented at ‘Hadrons 94’, Gramado, Brazil, April 1994, hep-ph/9407056.
15. M. Burkardt, Phys. Rev. D **54**, 2913 (1996).
16. H.-C. Pauli and S. J. Brodsky, Phys. Rev. D **32**, 1993 (1985); *ibid* 2001 (1985).
17. M. Burkardt, hep-th/9704162.
18. M. Burkardt and H. El-Khozondar, Phys. Rev. D **55**, 6514 (1997).
19. K.G. Wilson et al., Phys. Rev. D **49**, 6720 (1994).
20. M. Burkardt and A. Langnau, Phys. Rev. **D44**, 3857 (1991).
21. K.G. Wilson, Proc. 4th Int. Workshop on Light-Front Quantization and Non-Perturbative Dynamics, Ed. S.D. Glazek, (World Scientific, Singapore, 1994).
22. M. Burkardt, *to appear in Phys. Rev. D* hep-ph/9705224.
23. A. Casher and L. Susskind, Phys. Rev. D **9**, 436 (1974).